

CERN LIBRARIES, GENEVA

CERN/ISRC/77-24
26 October 1977



CM-P00048179

STATUS REPORT ON EXPERIMENT R-108

CERN¹-Columbia²-Oxford³-Rockefeller⁴ (CCOR) Collaboration

A. Angelis³, B.J. Blumenfeld², L. Camilleri¹, T.J. Chapin⁴,
R.L. Cool⁴, C. Del Papa¹, L. Di Lella¹, Z. Dimčovski⁴,
R.J. Hollebeek², D. Levinthal², L.M. Lederman², L. Lyons³,
N. Phinney³, S.H. Pordes¹, A.F. Rothenberg⁴, A.M. Segar³,
J. Singh¹, A.M. Smith¹, M.J. Tannenbaum⁴, R.A. Vidal²,
J. Wallace-Hadrill³ and T.O. White³

G E N E V A

1977

1. RECENT HISTORY

The superconducting solenoid was installed in the ISR tunnel during the August-October 1976 shut-down. The time between November 1976 and July 1977 was used for setting up. In particular, much time was spent in learning how to operate the cylindrical drift chambers in the 1.5 T magnetic field by taking data with different configurations of the electric fields in the chambers, different gas mixtures and different voltages on the sense wires. Some of the drift chamber modules were still being constructed.

By the end of the three-week shut-down which ended on 30 July, the drift chamber system was completed, and the working parameters finalized. Data-taking began on 1 August, using triggers sensitive to e^+e^- pairs, high- p_T π^0 's and π^0 pairs.

However, on 9 August a fault in the helium compressor caused some oil to contaminate the helium refrigerator, which stopped working. This accident has required a thorough cleaning of the refrigerating plant, including the addition of various filters. The refrigerator became operational again on 3 October, and data-taking with the magnetic field turned on was again possible from 22 October onwards.

2. PERFORMANCE OF THE DRIFT CHAMBERS

The drift chambers consist of four cylindrical modules (DC1-DC4), with the axis parallel to the magnetic field. Each module has two gaps, and the sense wires are parallel to the magnetic field \vec{B} . Thus the measurement of the drift time gives the position of a track point in a plane perpendicular to \vec{B} . The coordinate parallel to \vec{B} is measured simultaneously by delay lines located on the cathode planes in front of each sense wire. The time of the delay-line signal is measured at both ends of the delay line. The total number of sense wires in the system is 580.

A point in space is obtained by at least two out of the three possible signals from a sense wire and the corresponding delay line. Figure 1 shows the efficiency of the chambers for three values of the positive voltage applied to the sense wires. These efficiencies were measured at the ISR under normal running conditions with a luminosity of $\sim 2 \times 10^{31} \text{ cm}^{-2} \text{ sec}^{-1}$. In the case of the DC4 module, the 8% inefficiency appears to be associated with those tracks which cross the module at a distance of ≥ 15 mm from the sense wire. If this happens in one gap of DC4, the same track will then cross the other gap very close to the sense wire, since the sense wire positions are staggered in the two gaps of a same module, and hence will be detected efficiently.

Figure 1 suggests that the efficiency could be increased by an increase of the high voltage. However, this procedure results in electrical break-down somewhere in the chambers, and has so far been avoided.

The error in the measurement of the transverse momentum, $\Delta p_T/p_T$, depends on the track length L as L^{-2} . For tracks having at least one space point in DC1 and one in DC4, we expect $\Delta p_T/p_T = 0.8\% p_T \sigma$, where p_T is the transverse momentum in GeV/c and σ is the chamber resolution in a plane perpendicular to \vec{B} , measured in units of 0.1 mm. Requiring at least one point in DC1, one in DC4 and at least three points from the other two DC modules, gives a track reconstruction efficiency of 97.7%, under the pessimistic assumption that the two gaps of DC4 have independent efficiencies. In fact, the requirement of at least five space points corresponds to a track reconstruction efficiency of practically $\sim 100\%$, with 2.3% of the tracks being affected by an error $\Delta p_T/p_T$, which is ~ 2 times larger than the value quoted above.

However, in the course of the data-taking achieved so far, we have had some problems with faulty chamber sectors. This has limited the over-all track reconstruction efficiency so far achieved to about 80%, when averaged over the whole apparatus.

As already stated, these figures correspond to luminosities of $\sim 2 \times 10^{31} \text{ cm}^{-2} \text{ sec}^{-1}$. Recently, luminosities as high as $\sim 5 \times 10^{31} \text{ cm}^{-2} \text{ sec}^{-1}$ have been obtained in I-1, thanks to the low- β insertion, with excellent background conditions. During these runs, the chambers could not be tested with the magnetic field turned on because of the fault of the refrigerator mentioned above. The only consequence of a higher luminosity should be the larger number of space points recorded, resulting from accidental events occurring within the sensitive time of the electronics. The coordinates of the points from accidental tracks, however, are wrongly calculated, since the drift times are measured from the time at which the trigger occurred. Unless the track belongs to an event which occurred within ~ 50 nsec from the triggering one, no track will be reconstructed from these points.

On the grounds of these considerations, we believe that the present system will work well up to luminosities around $10^{32} \text{ cm}^{-2} \text{ sec}^{-1}$.

Finally, as already reported to the ISRC during the Open Meeting of 8 June 1977, we have measured an intrinsic chamber precision $\sigma = 0.275$ mm in a plane perpendicular to \vec{B} , and $\sigma = 4$ mm for the coordinate parallel to \vec{B} . The value $\sigma = 0.275$ mm would result in an error $\Delta p_T/p_T = 2.2\% p_T$ (p_T in GeV/c). However, we have not yet reached this precision in practice, due to slight misalignments of the chambers and to inadequate knowledge of the track distance from a wire, as a function of the measured drift time and track angle. The present error $\Delta p_T/p_T$,

averaged over the entire detector is $\approx 4\% p_T$ (p_T in GeV/c). It will improve through better chamber alignment and a better understanding of the drift properties. A new precise survey of the chamber positions was recently performed during the October shut-down, and studies of the drift properties of our chambers are in progress, using both the data and a special laboratory set-up. It should be pointed out that the survey of the chambers is only possible during a long (≥ 2 weeks) ISR shut-down.

3. PHYSICS WITH HIGH- p_T π^0 'S

Preliminary results obtained on the inclusive production of π^0 's at $\sqrt{s} = 52.7$ and 62.4 GeV were presented at the recent Workshop on Future ISR Physics. They are shown here in Figs. 2 and 3, where they are compared to previous data. The data clearly show the potentiality of the apparatus to reach p_T values as high as 13 GeV/c or even higher. A careful investigation of the various background sources that could contribute to the observed events is in progress.

Another important aspect in the study of inclusive π^0 production is the lead-glass calibration. As it is known, our lead-glass counters need to be recalibrated once every year or so, and the last calibration was performed early in 1976. We had originally planned a new calibration at the end of the present year, but, given the fault in the refrigerator mentioned above, we are eager to take a good amount of data with the whole apparatus working as soon as possible. Hence we have decided to postpone this calibration to early in 1978.

With all of the drift chambers working and the magnetic field turned on, it is possible to study the correlations between a high- p_T π^0 and the charged particles produced together with it. Previous studies on this subject had been limited to $p_T(\pi^0) < 4$ GeV/c, and had used detector system (the split-field magnet) whose acceptance is far from being uniform over the full azimuth.

We have just started the analysis on this subject, again using the data taken at the beginning of August. Examples of some of the results are displayed in Figs. 4-6. Figure 4 shows the azimuthal correlation between a high- p_T π^0 and the charged particles, for various intervals of $p_T(\pi^0)$. Tracks with $p_T < 1$ GeV/c have been excluded, to reduce the background from the "normal event". The data clearly show the opposite side "jet" observed at lower values of $p_T(\pi^0)$, with very little background elsewhere. For $p_T < 9$ GeV/c, a peak centred at the same azimuth as the π^0 is also visible.

Figure 5 shows the average value of p_{out} as a function of $p_T(\pi^0)$, for the charged particles detected in the opposite hemisphere. As it is known, a limited value of p_{out} is considered to be an indication for jet production. Figure 5

shows that even at $p_T(\pi^0)$'s as high as 10 GeV/c, p_{out} continues to be limited. In addition, its value (~ 0.5 GeV/c) is in good agreement with the values found in other experiments at much lower values of $p_T(\pi^0)$.

Finally, Fig. 6 shows the p_{out} distribution for the events with $p_T(\pi^0) > 6$ GeV/c.

The analysis of the correlation between two high- p_T π^0 's, which is also studied in our experiment, is in progress.

Given a total running time of 1000 hours at $\sqrt{s} = 52.7$ GeV, with a luminosity of $4 \times 10^{31} \text{ cm}^{-2} \text{ sec}^{-1}$, 600 π^0 's with $p_T > 13$ GeV/c will be recorded. Approximately the same number is expected for 1000 hours of running time at $\sqrt{s} = 62.4$ GeV, with a luminosity of $2 \times 10^{31} \text{ cm}^{-2} \text{ sec}^{-1}$. Both these luminosity values have been obtained using the low- β scheme in I-1, with excellent background conditions.

We think that an equal sharing of the running time between 52.7 and 62.4 GeV during 1978 is reasonable, in order to study the s -dependence of π^0 production at the very high values of p_T which can be reached. In particular, it will become possible to study the behaviour of the exponent n as a function of x_T in the relation

$$E \frac{d^3\sigma}{dp^3} = p_T^{-n(x_T)} f(x_T) , \quad (1)$$

in order to detect possible deviations from the value $n \approx 8$ found in previous experiments. As will be seen in Section 4, equal sharing of the running time between 52.7 and 62.4 GeV is also required in the study of e^+e^- production. It will also be necessary to have some time ($\approx 10\%$) at a lower c.m.s. energy ($\sqrt{s} = 30.6$ GeV), to check the validity of parametrization (1) in π^0 production. Here we note that large x_T values are more accessible at lower values of s , and we do not need to exceed values $p_T(\pi^0) \gtrsim 8$ GeV/c at $\sqrt{s} = 30.6$ GeV. The operation of the low- β scheme at $\sqrt{s} = 30.6$ GeV would reduce the actual running time of the ISR at this energy, through a corresponding increase in luminosity. In addition, the ability to operate the solenoid at this energy would be highly welcome.

4. ELECTRON PAIRS

The data accumulated on tape before the break-down of the refrigerating plant amounts to an integrated luminosity of $9 \times 10^{36} \text{ cm}^{-2}$. Using FNAL results and Drell-Yan scaling, this should yield about six e^+e^- pairs of mass greater than 6 GeV/c² from the continuum and two or three T's.

These data are currently being analysed and the following cuts are being applied in order to reject hadron pairs:

- i) A track of momentum $p > 1$ GeV/c pointing to a cluster of energy in the lead-glass.
- ii) A pulse height in the B counters (located outside the solenoid), larger than that corresponding to 1.5 single ionization.
- iii) A pulse height in the A counters (surrounding the intersection region) less than that corresponding to 1.5 single ionization. This rejects Dalitz decays and conversions in the ISR vacuum chamber.

In addition, the total transverse momentum p_T of the pair is required to be less than 2.25 GeV/c.

Figures 7a-7d are plots of the invariant mass of e^+e^- candidates for various cuts on the data. The mass is calculated using the energy measurement in the lead-glass and the resulting mass resolution is estimated to be 0.93 GeV (FWHM) at a mass value of 10 GeV.

The predicted yield of e^+e^- pairs per GeV from the continuum, scaled up to ISR energies from the recent Fermilab data of Herb et al., is shown in Fig. 8 for 1000 hours of running time at luminosities of $4 \times 10^{31} \text{ cm}^{-2} \text{ sec}^{-1}$ at $\sqrt{s} = 52.7$ GeV, and $2 \times 10^{31} \text{ cm}^{-2} \text{ sec}^{-1}$ at $\sqrt{s} = 62.4$ GeV, respectively. It is clear that at $\sqrt{s} = 52.7$ GeV, the yield is larger for masses below 15 GeV. For masses above 15 GeV, $\sqrt{s} = 62.4$ GeV should be preferred. However, the yield is very small (< 1 event per GeV \times 1000 hours) at masses above 15 GeV. These conclusions are valid for the continuum, and do not take into account the possible existence of new, as yet undiscovered, heavy resonances. This last exciting possibility leads us to request equal sharing of running time between $\sqrt{s} = 52.7$ and $\sqrt{s} = 62.4$ GeV during 1978.

5. FUTURE PLANS

It is planned to add two multiwire proportional chambers (MWPCs) to the present apparatus, to be located just in front of the lead-glass arrays, one on each side of the intersection region. Each MWPC has two cathode planes consisting of 0.8 cm wide strips, oriented horizontally and vertically, respectively. A system of ADCs will be used to measure the pulse height of the signals induced on the strips, so as to identify electromagnetic showers emerging from the solenoid cryostat and coil.

The purpose of these MWPCs is twofold:

- i) to provide further rejection against hadrons in the study of e^+e^- pairs, by making use of the different space distribution of a hadronic cascade with respect to an electron shower;

ii) to improve the space resolution for photons, which is at present limited by the size of the B counters and of the lead-glass blocks.

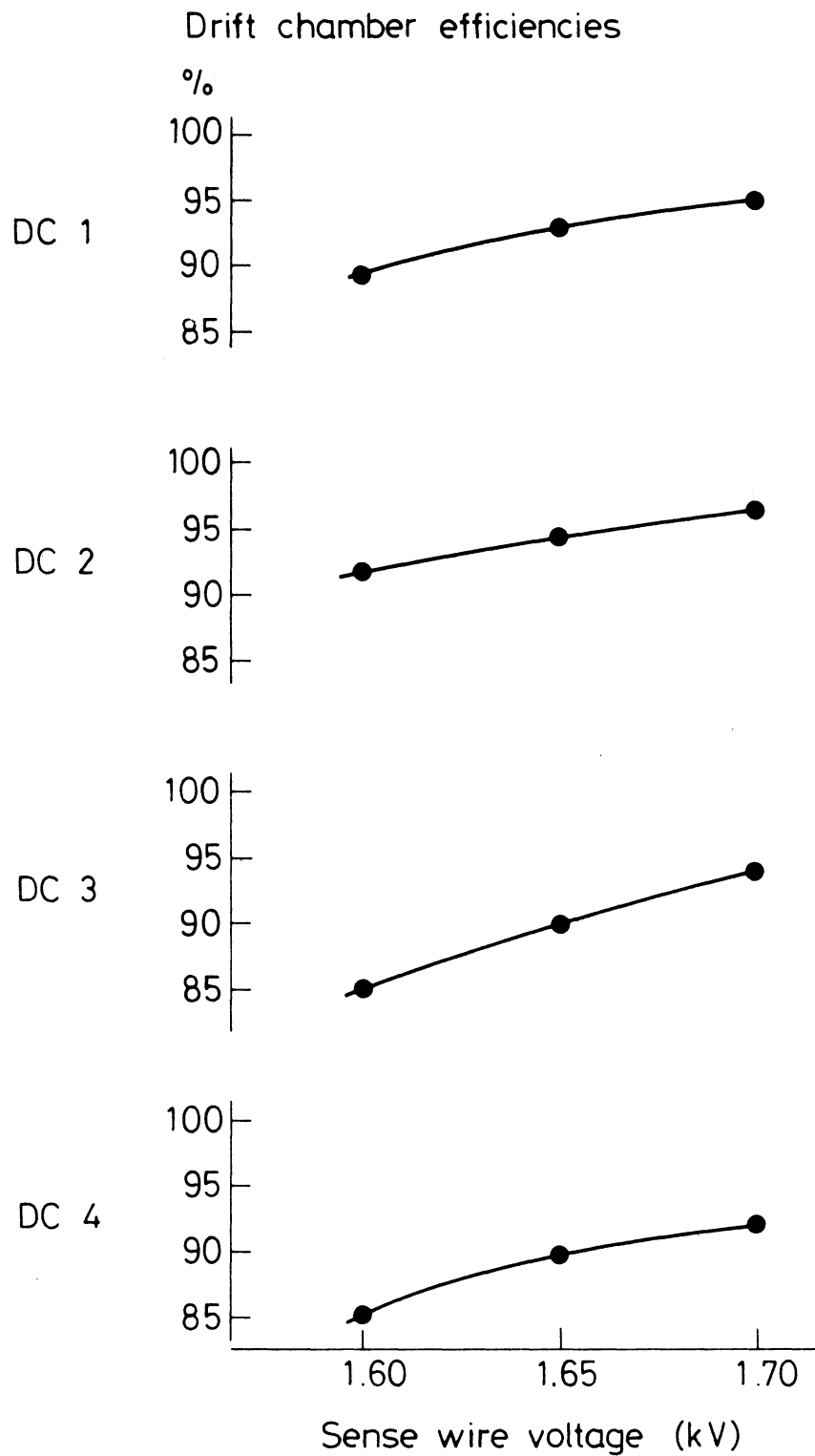
A small prototype of such a MWPC has been successfully tested at the PS during the present year. A larger size MWPC is being constructed in Oxford, and will be shipped to CERN during the month of November to undergo tests at the PS. The construction of the final modules, which will have a sensitive area of 210×180 cm and which will total ~ 1000 strips, will begin in Oxford as soon as the tests on the second prototype are completed. The ADCs are being developed and constructed at Columbia.

It is expected to add the two final modules to the present apparatus during the summer of 1978.

A further addition to the apparatus for the not-so-near future could be a fast hardware processor (called a "black box") which reconstructs the tracks from the drift chamber information in the solenoid and measured their momentum in less than 1 msec. Such a black box, with the addition of the information from the lead-glass, would then provide the possibility of triggering on jets, defined as a system of hadrons (including π^0 's) with a large total transverse momentum. The black box is being studied at present by W. Sippach at Columbia and it could be available in the first half of 1979.

Figure captions

- Fig. 1 : Drift chamber efficiencies.
- Fig. 2 : Invariant cross-section for inclusive π^0 production at $\sqrt{s} = 52.7$ GeV.
- Fig. 3 : Invariant cross-section for inclusive π^0 production at $\sqrt{s} = 62.4$ GeV.
- Fig. 4 : Azimuthal correlations of charged particles with $1.0 < p_T < 5.0$ GeV/c, with a high- p_T π^0 .
- Fig. 5 : Average value of p_{out} for charged particles with $1.0 < p_T < 5.0$ GeV/c, emitted in the opposite hemisphere to a high- p_T π^0 , as a function of the π^0 transverse momentum.
- Fig. 6 : Distribution of p_{out} for charged particles with $1.0 < p_T < 5.0$ GeV/c, emitted in the opposite hemisphere to a π^0 with transverse momentum between 6 and 10 GeV/c.
- Fig. 7 : Invariant mass distribution of e^+e^- pairs for various cuts to the data.
- Fig. 8 : Expected number of e^+e^- pairs/GeV at $\sqrt{s} = 52.7$ GeV and 62.4 GeV, respectively, for 1000 hours of running time.



$B = 1.5 \text{ T}$, $\sqrt{s} = 52.7 \text{ GeV}$, high luminosity

Fig. 1

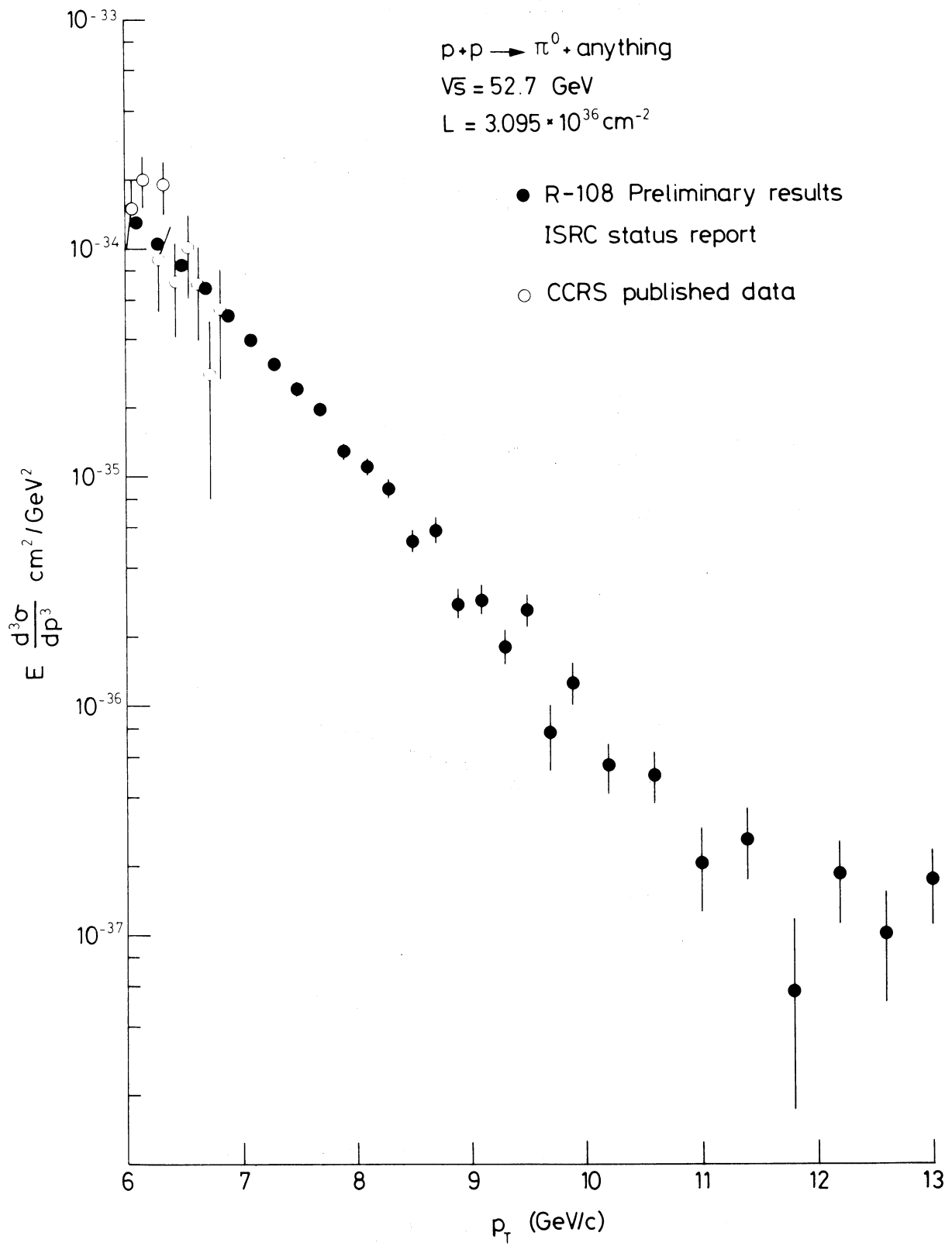


Fig. 2

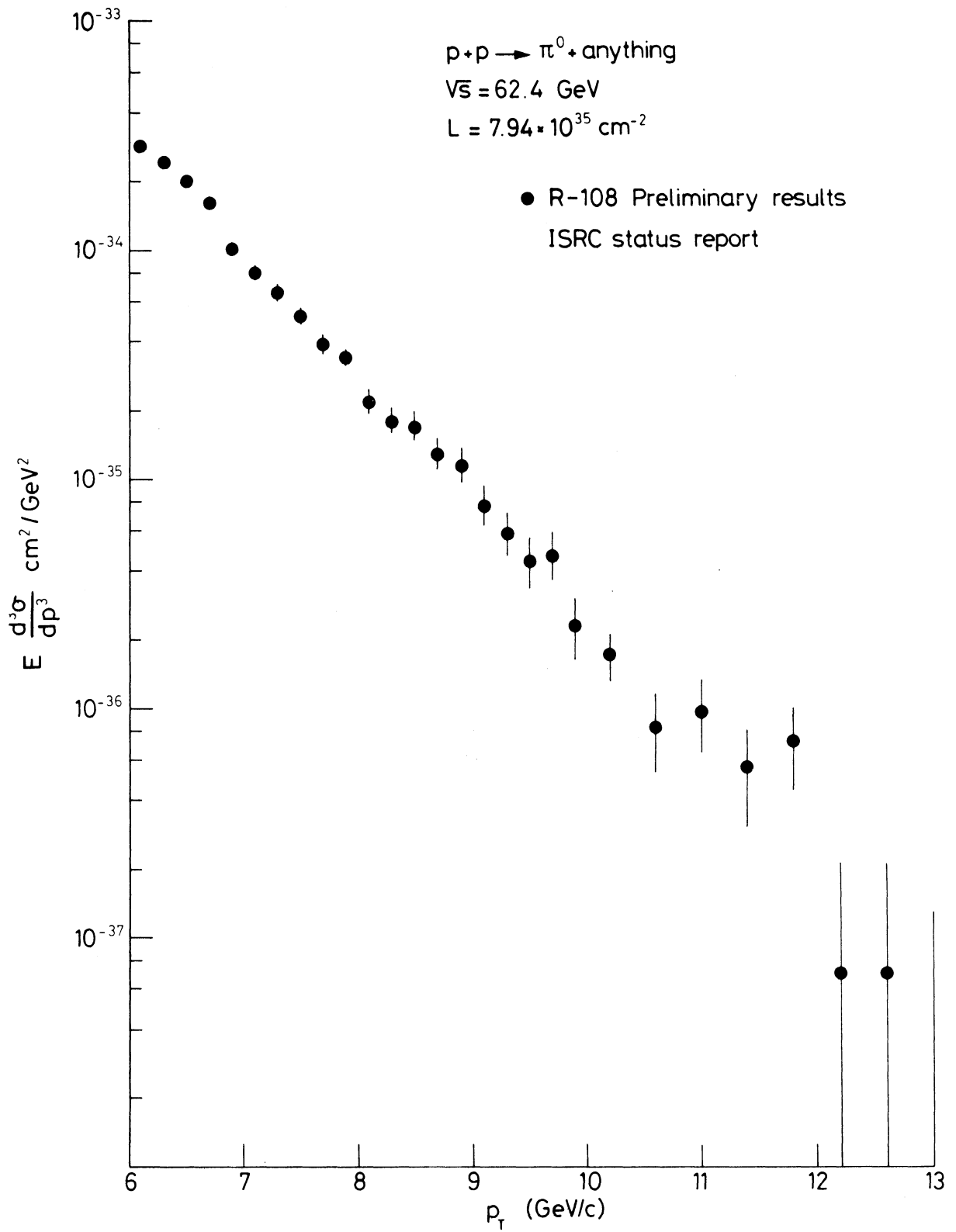


Fig. 3

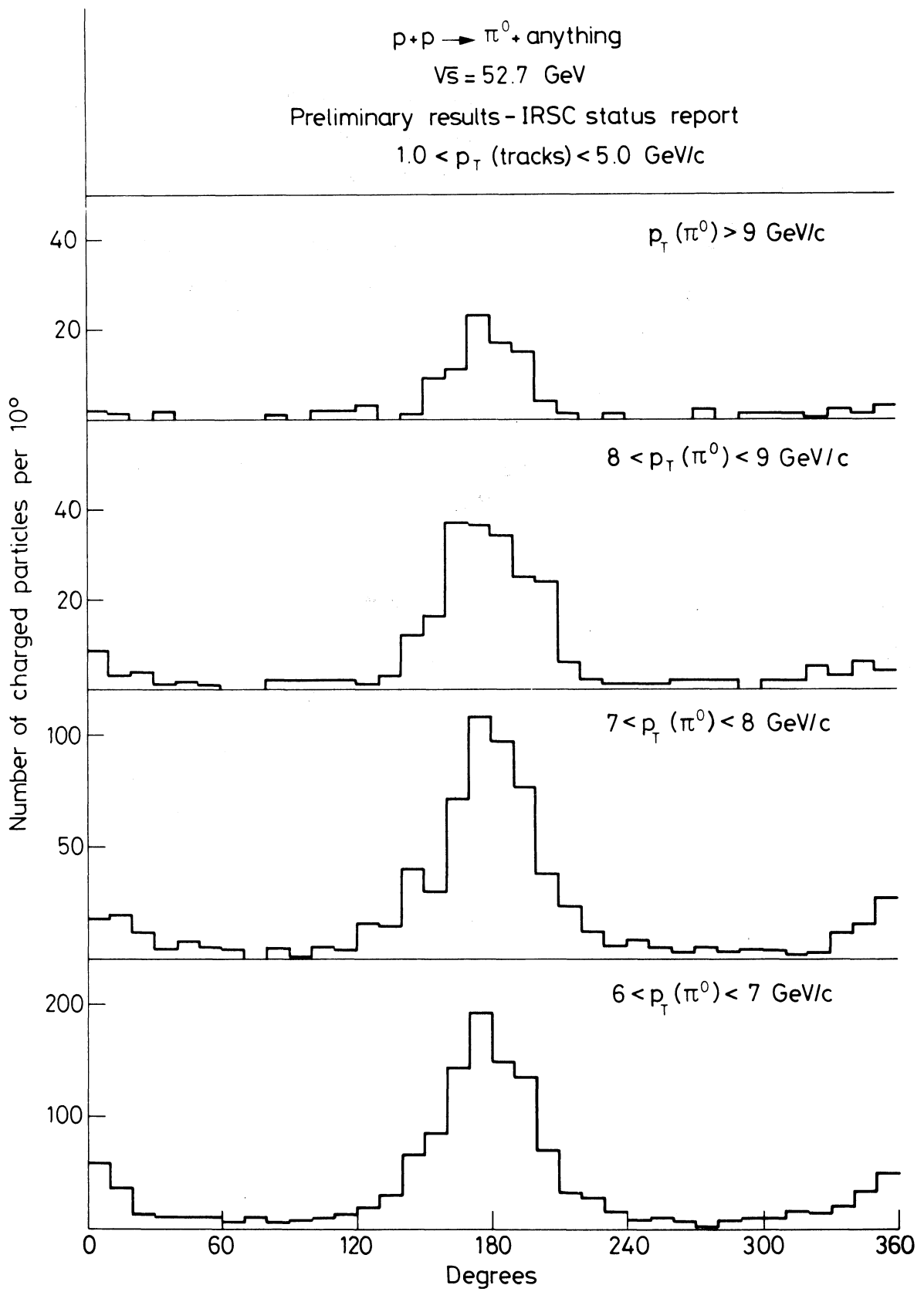


Fig. 4

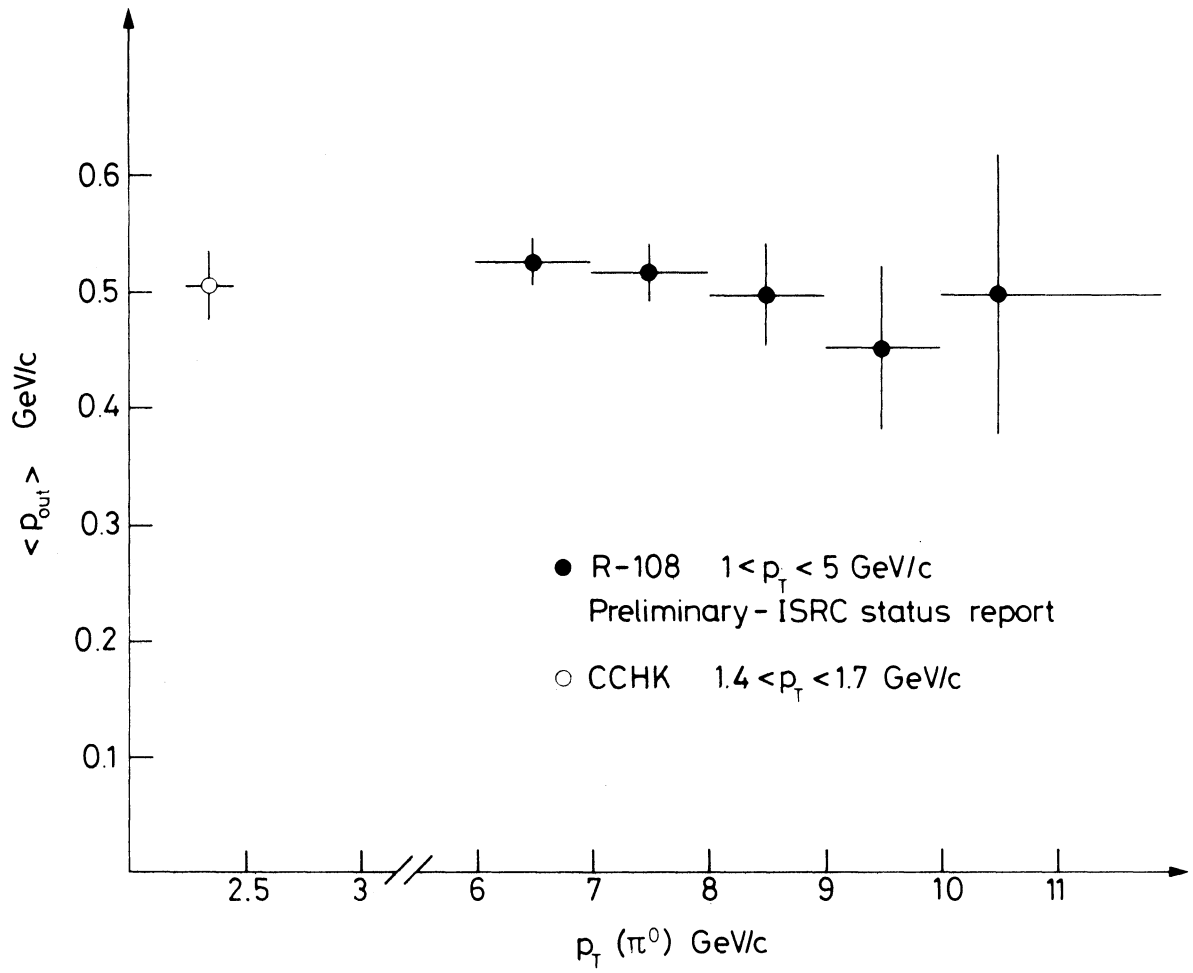


Fig. 5

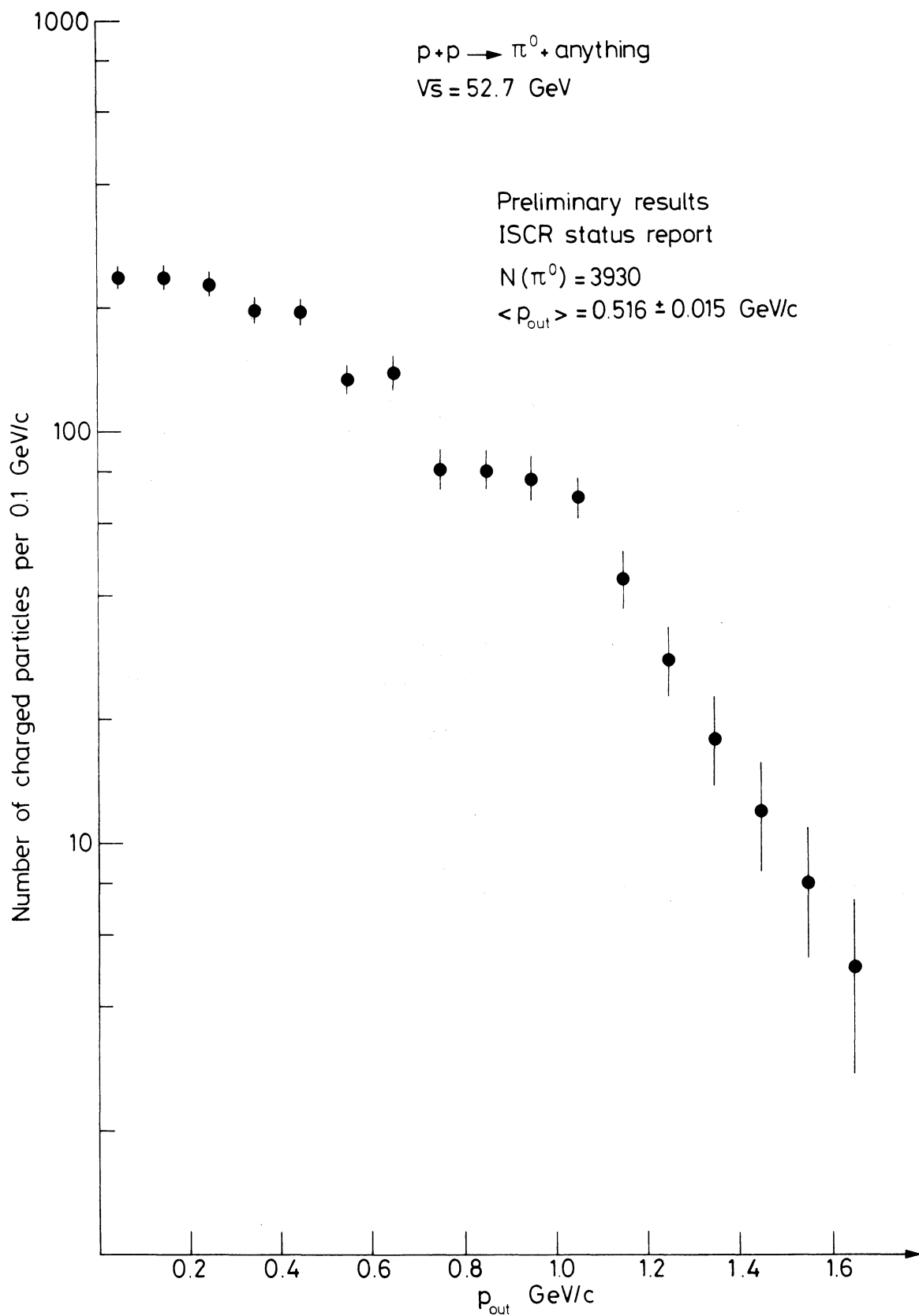


Fig. 6

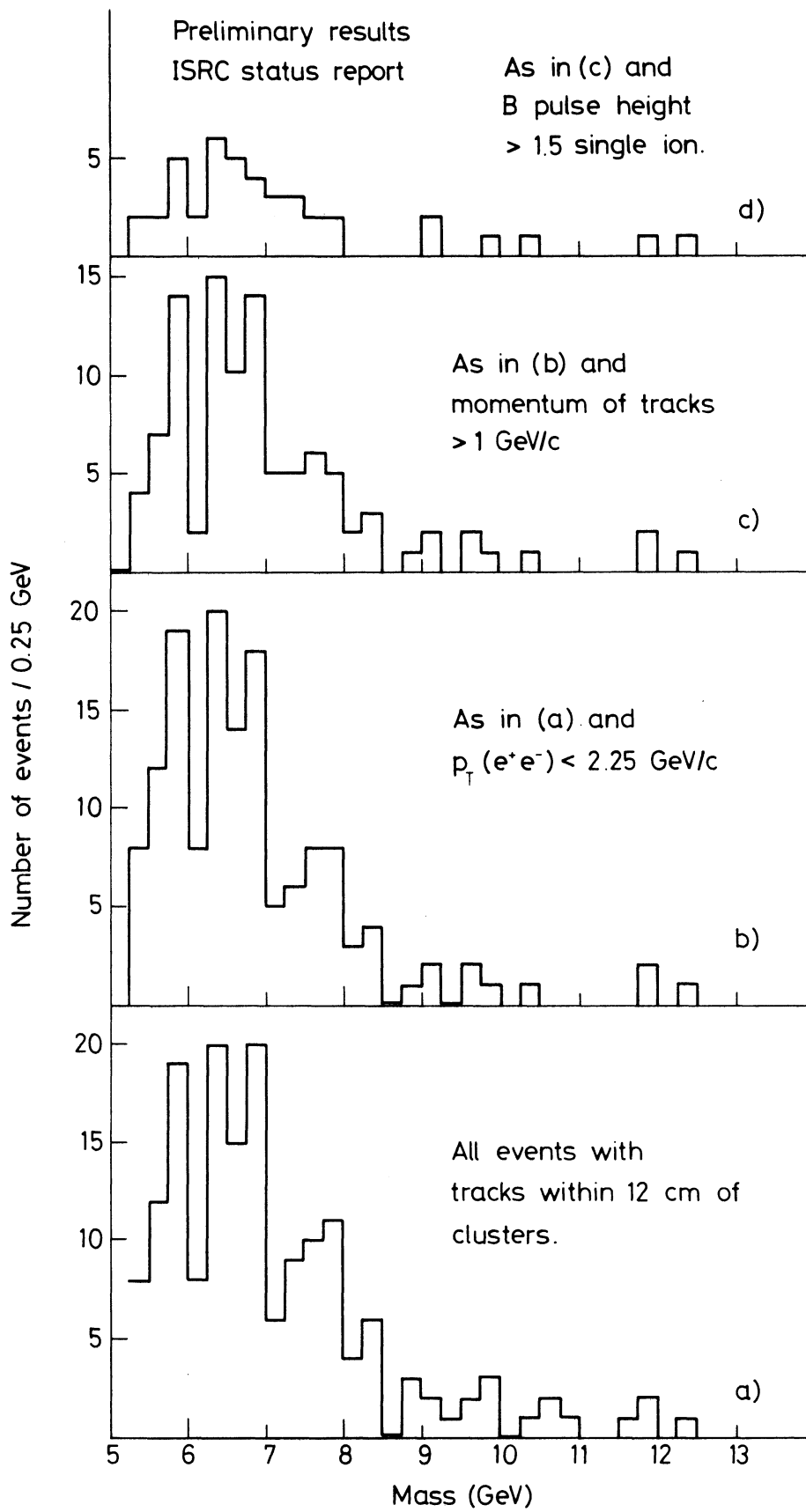


Fig. 7

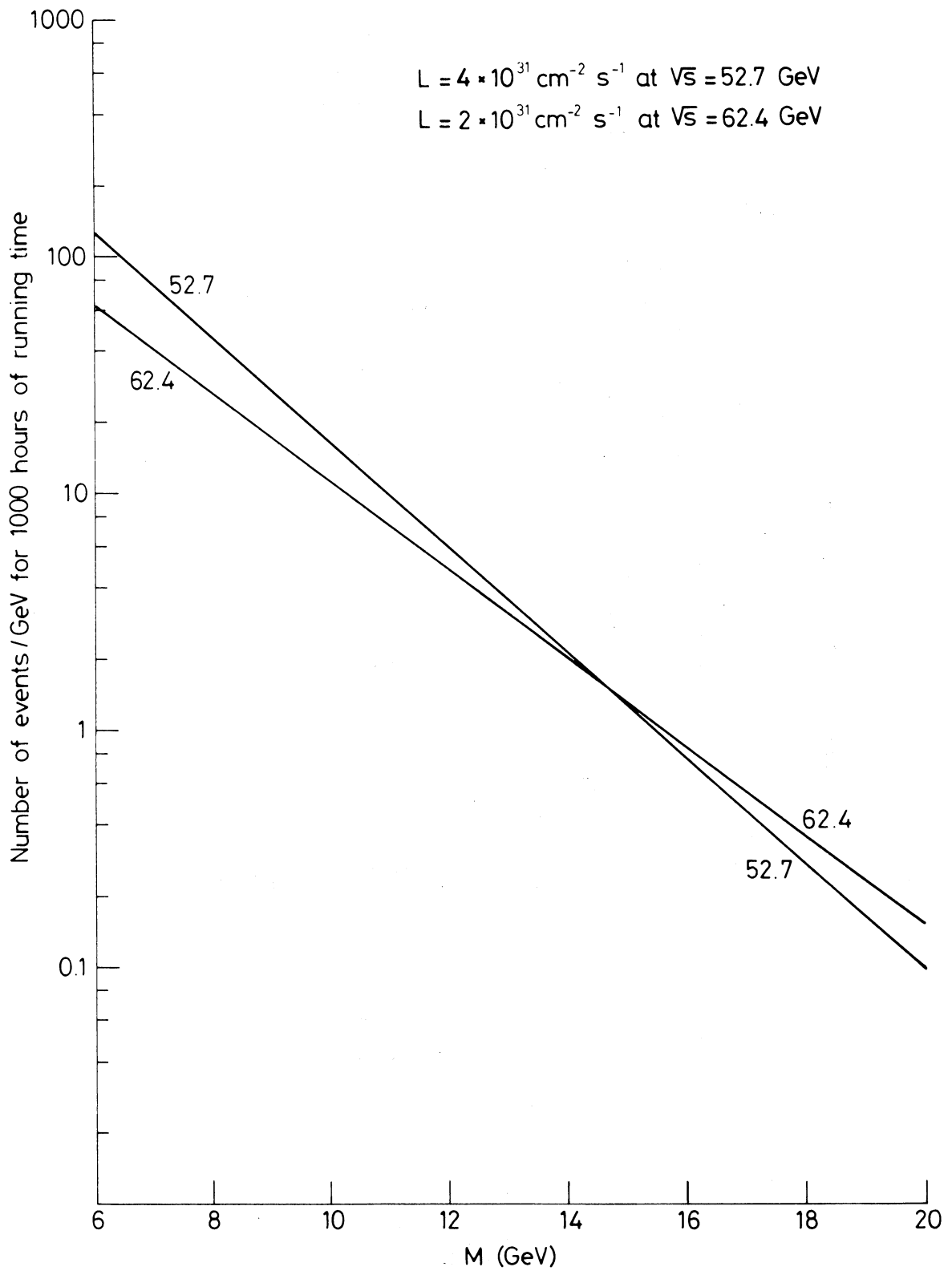


Fig. 8